ORIENTATION AND ALIGNMENT OF THE $3P^3P_{2,1,0}$ STATE OF NEUTRAL HELIUM DUE TO NEAR GRAZING COLLISIONS WITH AN ALUMINUM TARGET

A Thesis

by

GEORGE ROBERT WELCH

Submitted to the University Undergraduate Fellows Program of

Texas A&M University

in partial fulfillment of the requirements of the program

23 April 1979

Major Subject: Physics

Thesis Advisor

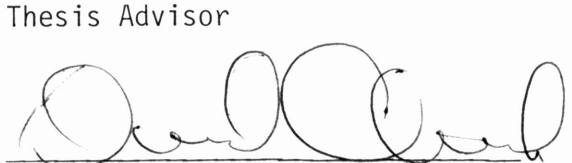

Dr. David A. Church

ABSTRACT

Polarization measurements of light emitted near 3889 Å from fast He atoms, resulting from near grazing collisions with an aluminum target by incident 1--9 keV He^+ ions are described. The polarization results were analyzed in terms of the Stokes' parameters, and related to the $3p\,^3P_{2,\,1,\,0}$ upper excited level anisotropy using orientation and alignment parameters. The results are compared to those of other researchers and are analyzed using a classical model of the charge capture process leading to circularly polarized radiation. The ion source, accelerator, vacuum system, and photon counting system that were designed and built for this research are described.

ACKNOWLEDGMENTS

I would like to express my deepest possible appreciation to Dr. D. A. Church. He has been more than simply an advisor to me; perhaps motivator or mentor would be more indicative of his role. The guidance, assistance, concern, and friendship which he has shown over the past two years will be an eternal source of pride for me, and it is my sincere hope that as my career continues I shall be able to give at least partial justification for him to reciprocate this feeling.

I would also like to thank Dr. Melvin Friedman for the University Undergraduate Fellows Program. I think it will suffice to say that for me it has been all he would have wanted, at the very least. It has indeed, "challenged me to the utmost".

I would also thank Chin Lee for his help in practical laboratory matters and John Welch for his part in the design of the accelerator and lens system. I also thank Jim Swede, the physics department machine shop foreman, for his perseverance and patience.

Finally, I would like to express great appreciation to those responsible for this thesis requirement. It has, more than anything else, taught me the dire consequences of procrastination.

TABLE OF CONTENTS

LIST OF FIGURES

INTRODUCTION

Anisotropy of the spatial distribution of angular momentum in the excited state of an atom or ion is described by an orientation vector and an alignment tensor. This anisotropy appears in the polarization state of the light emitted by the excited atoms during radiation. By measuring the polarization state of the light emitted in transitions at characteristic wavelengths from atoms which have been excited during collisions with a target, the orientation and alignment parameters of the excited atom states can be found. To completely determine the orientation and alignment of an excited state, one must be able either to measure the polarization fractions and the total intensity of the light emitted, or to make measurements of the polarization fractions of the light emitted in more than one direction. Total completion of either of these procedures was beyond the scope of this research program. However good estimates can be made for the orientation and alignment parameters by measuring only the polarization fractions of the emitted radiation in a direction normal to the incident beam and parallel to the target.

I was interested in determining if the excited levels of fast helium atoms produced by charge capture collisions with a solid surface at low (< 10 keV) energies were either aligned or oriented by such a collision. Such collisions were known to produce both orientation and alignment at energies greater than 15 keV. At the beginning of this project no research of this type had been conducted for any incident projectile in the range of incident ion energies below 15 keV.

Collisions of ions with atoms or molecules in a foil or gas have cylindrical symmetry about the beam axis, and linearly polarized light can be emitted by either the projectile or target particles. This linear polarization provides a measure of the incoherent population of the magnetic sublevels of the states of the ions or atoms which were excited during the collisions. In this case the linear polarization is characterized by the Stokes parameter $M = (I_o - I_{90})/(I_o + I_{90})$ where the subscripts indicate the polarization angle relative to the beam axis.

Only in collisions which depart from cylindrical symmetry about the beam axis can coherent alignment or orientation of these sublevels occur. This effect has not been studied in ion-atom collisions and has only recently been observed in ion solid collisions. Coherent alignment and orientation of the excited states are respectively characterized by 45 degree linear polarization and circular polarization of the emitted light. These coherent effects are thought to be associated with electric fields from the surface of the solids which shift the phase of the excited wave function substates. The fields are near the surface so that the phase shifts are related to collision time, and hence to the reciprocal of the collision velocity. The magnitude of such phase shifts should be greatly different between high energy MeV collisions and the collisions studied here with keV energies.

The apparatus needed in order to perform the measurements consists of an ion source, ion optical system, and accelerator; a collision chamber with a target; and an optical system and associated electronics for collecting and analyzing the radiation. I have designed and built an

ion source and accelerator with a vacuum system capable of maintaining pressures low enough to sustain an ion beam. Without extensive ultra-high vacuum equipment necessary for maintaining a clean target surface, one must tolerate the presence of a layer of gas atoms on this surface. Nonetheless, meaningful results can be obtained even in the presence of the layer of gas atoms. With limited resources only a modest target chamber could be assembled. This chamber permitted the observation of deexcitation radiation only in a single direction perpendicular both to the target normal and to the beam, but this was sufficient to complete the measurements outlined above. An optical system was assembled with a wavelength resolution sufficient to isolate characteristic helium transitions, and measure and characterize their polarization using individual photon counting techniques. The data from these measurements are analyzed using recently developed theoretical descriptions, and are compared with measurements made at other energy ranges and with different projectiles.

THE APPARATUS

1. The Ion Source

The ion source is a duoplasmatron based principally on that of A. R. Hill[1]. The ion exit piece was designed with reference to a duoplasmatron by R. Becherer et al[2], who also furnished detailed information of the effect of the axial magnetic field on the efficiency of production of the ion beam.

Gas enters the ion source from a glass tube (see figure 1) which can be opened and closed with a stopcock. No vacuum problems were encountered owing to the relatively high pressure in the ion source. While the data presented in this thesis was all taken with a source pressure of 250 mT for consistency, operation of the source was tested for pressures in the range of about 70 to 2000 mT. The only effect of this variation in source pressure was an increase of the ion beam current, which rose slightly with the source pressure, leveling off at approximately 200 mT. The effect of variations in the source pressure on the pressure in the target chamber could not be accurately determined experimentally. The thermocouple type gauges used in the apparatus are effective in the range of 1-2000 mT, which is entirely above the pressure that was maintained in the target chamber. However, a simple calculation will suffice to give an idea of the relationships of the parameters, and provide a crude estimate quantitatively. Figure 2 provides a schematic for the calculation. Denote the pressure in the source by P_s, the pressure in the chamber by P_c, the conductance through the ion exit piece by C and the pumping speed of the pump by S. at equilibrium

$$(P_s - P_c)C = SP_c$$

FIGURE 1

The Duoplasmatron Ion Source

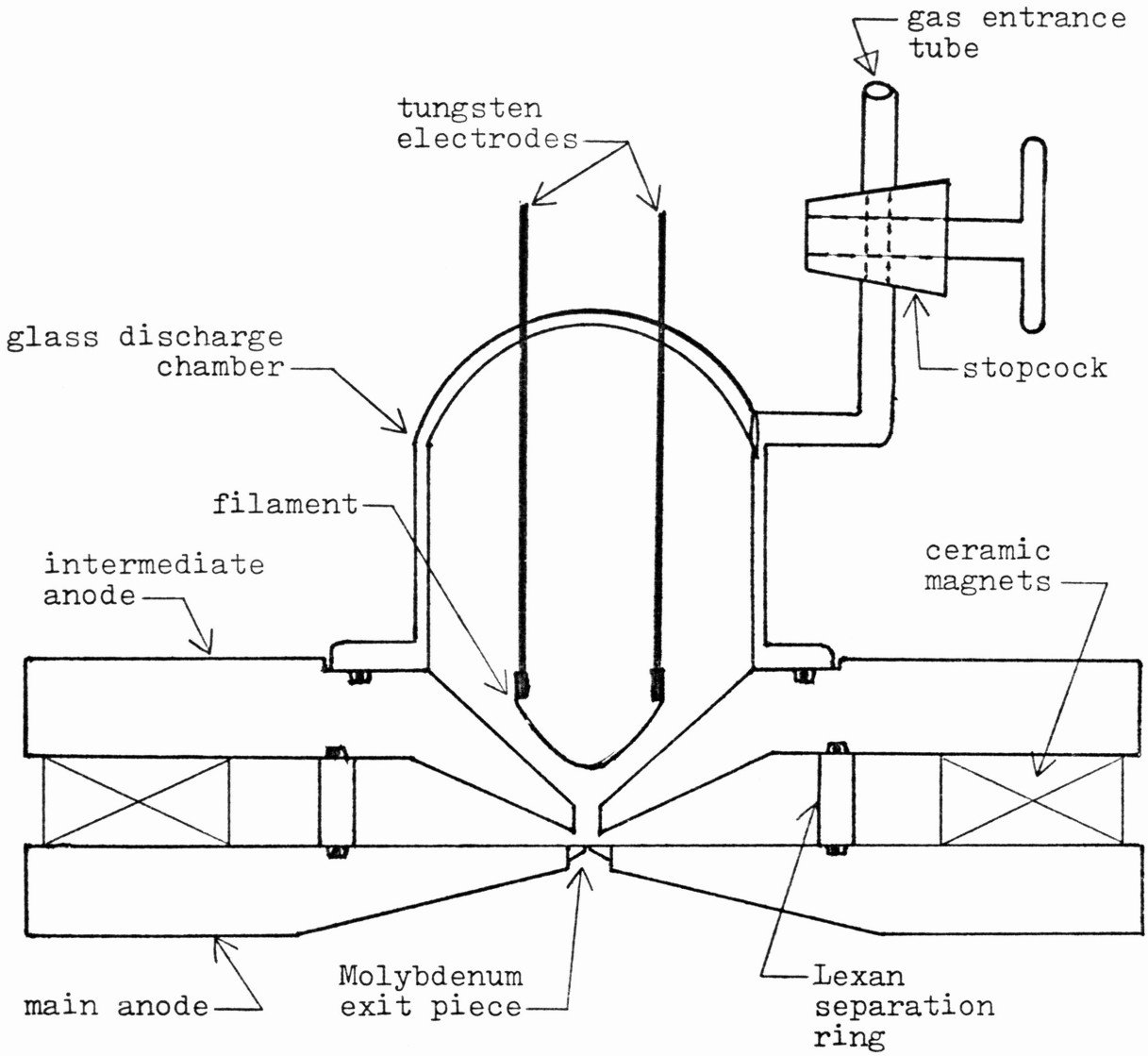

or since $P_c << P_s$

$$P_s C = S P_c$$

so

$$P_c = P_s C/S.$$

Hence the chamber pressure varies linearly with the source pressure over the ranges being considered. The conductance of the ion exit piece can be estimated from $C = 80\ D^2$ where D is the aperture diameter in inches and C is in liters/second. The pumping speed of the diffusion pump is 105 l/s, giving

$$P_c = 2 \times 10^{-4}\ P_s.$$

For P_s = 250 mT we obtain $P_c = 5 \times 10^{-5}$ torr. While this pressure is high, it could be lowered at most by a factor of 3 or 4 by decreasing the source pressure by the same factor. As already pointed out, this would lower the ion beam current, and the trade-off was determined to be unadvantageous. With this reasoning, the source pressure was maintained at 250 mT during data collection.

The lifetime of the tungsten filament was relatively unaffected by the source pressure, which is reasonable since the only gas used was helium. It is interesting to note that the filament lifetime was quite short, being only about 6 hours under normal operation. The filament (diameter = .010 in.) was connected to two tungsten electrodes which enter from the back of the glass discharge chamber. Connection of the filament to the electrodes could not be accomplished directly by spot welding them, as tungsten does not readily spot weld to tungsten. Instead, an indirect method was used. The filament was spot welded to small platinum tabs, which could be spot welded in turn to the tungsten

electrodes. This method also facilitated changing the filament, because the spot welds of the platinum tabs to the electrodes could be easily broken without endangering the seals of the electrodes in the glass discharge chamber. The filament was heated with 5-7 Amps. The amount of current needed decreased as the filament life increased, indicating a significant reduction in diameter due to sputtering.

The idea behind the double anode arrangement of the duoplasmatron is to confine the discharge in the small region between anodes in front of the ion exit piece. Confining the discharge to this region concentrates ion production there, which increases extraction efficiency. The resistor arrangement on the discharge power supply output lines puts a greater voltage on the main anode than on the intermediate anode, concentrating the discharge as desired. This effect was readily seen by observing the spatial distribution of light emitted by the discharge during operation. The probabilities of excitation and ionization are related, so light emission gives a measure of ionization. A fixed discharge potential of 140 Volts was used during operation. Since the parallel impedence of the two anode resistors was not high enough to insure a stable discharge current for the voltage desired, the series 300 ohm resistor was inserted into the circuit. With a typical discharge current of 175 mA, 60 volts were on the main anode and 10 volts were on the intermediate anode, with repect to the filament.

Confining the discharge in this region is useful but not sufficient to properly contain the produced ions in front of the exit piece. To confine the ions radially, an axial magnetic field is applied with a series of ceramic magnets between the iron anodes, with their poles

against them. This field confines the ions in cyclotron orbits around the axis, which prevents their spreading outward due to radial electric fields or thermal motion. Measurement of the magnitude of the magnetic field is complicated by the apparatus geometry and has not yet been done, but source operation indicates that the magnitude of the field is sufficient.

Since the anodes must be electrically isolated, no metal bolts could be used to give them mechanical stability. This presents no problem when the source is evacuated since air pressure holds them in place. Otherwise, the magnets proved adequate the rest of the time so no other effort was made to secure the anodes with respect to one another. However the ceramic magnets are not totally non-conducting and thin teflon sheets were used to insure that there was no leakage across the anodes.

The discharge power supply was a Hewlett-Packard model 712B. The filament power supply was an NJE model SY 36-30.

The ion exit piece (see figure 3) is made of molybdenum and fits into the main anode as shown. Molybdenum was used since it is at the center of the discharge, and being a refractory metal does not sputter easily. However noticeable wear due to sputtering occured, and after less than 50 hours of operation the exit piece resembled figure 4. Originally, a hole diameter of .008 inches was used in the exit piece. The major problem was in pumping out the ion source. The only throughput from the source into the main pumping region is through the hole in the ion exit piece. When the hole diameter was increased to .016 inches, significantly lower pressures were obtained in the ion source. It is

FIGURE 2
Diagram for Pressure Calculation

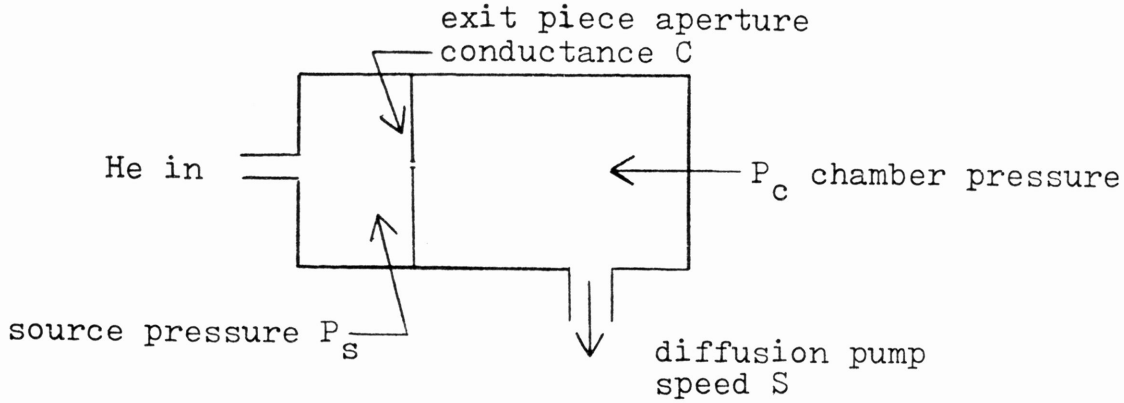

FIGURE 3
Ion Exit Piece

The exit piece fits snugly into main anode, flush with its surface.

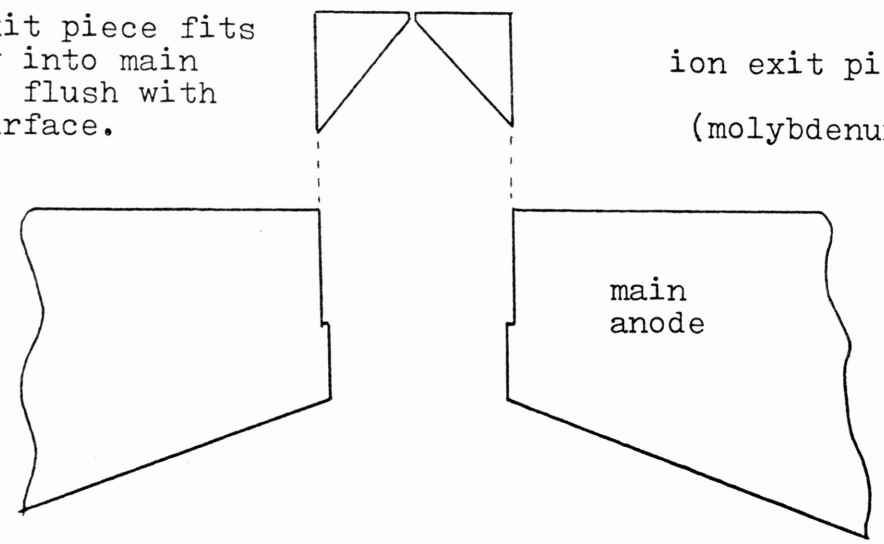

FIGURE 4

Enlarged view of exit piece showing wear due to sputtering.

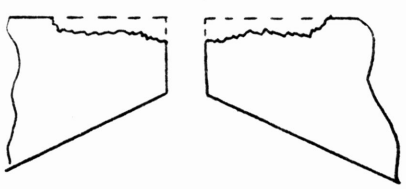

also interesting to note that during operation of the beam, the process of ion extraction could reduce the pressure in the ion source. Drops in pressure of up to 20% were noticed immediately following the application of extraction voltage, indicating the ions make up a significant portion of the gas in the ion source during operation, and transfer significant energy to the gas atoms by elastic collisions.

The extraction voltage was provided by a Hipotronics model R15B high voltage power supply. For the reasons of safety and convenience the down beam region of the accelerator was held at ground, and the ion source was floated at the extraction voltage (see figure 5). The negative terminals of both ion source power supplies were grounded to their cases, which in turn were connected to the posivive output terminal of the extraction power supply with the negative terminal grounded. This arrangement could be reversed in polarity if desired, to accelerate negative ions. Only positive ions were accelerated in the research covered by this thesis. It was then necessary to isolate the discharge power supplies with the 1:1 isolation transformer on their input lines as shown. The power supplies were mounted in a wooden rack and closed in front with a 1/4 inch clear lucite cover. Adjustments could then be made with lucite rods through openings in the cover without danger to the operator. (see figure 6)

2. Accelerator and Lens

Extracting and accelerating the ions was accomplished with a single conical electrode as shown in figure 7. This electrode was made of aluminum and was grounded through the adjustment mechanism. Its position could be adjusted from .15 to 1.75 inches from the ion exit hole in

FIGURE 5
Electrical Schematic of Ion Source and Accelerator

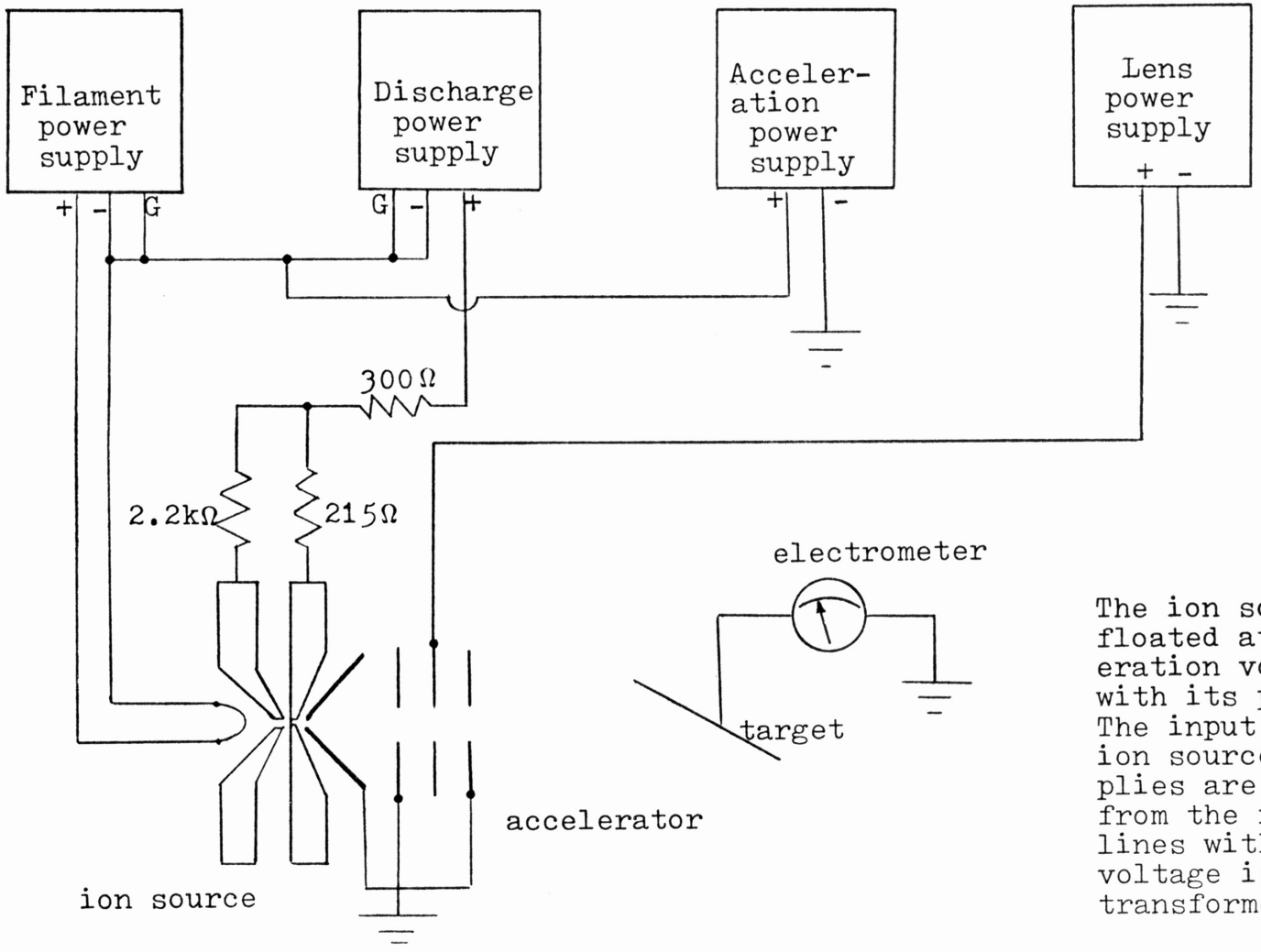

The ion source is floated at the acceleration voltage along with its power supplies. The input lines of the ion source power supplies are separated from the room power lines with a 1:1 high voltage isolation transformer.

FIGURE 6
High Voltage Safety

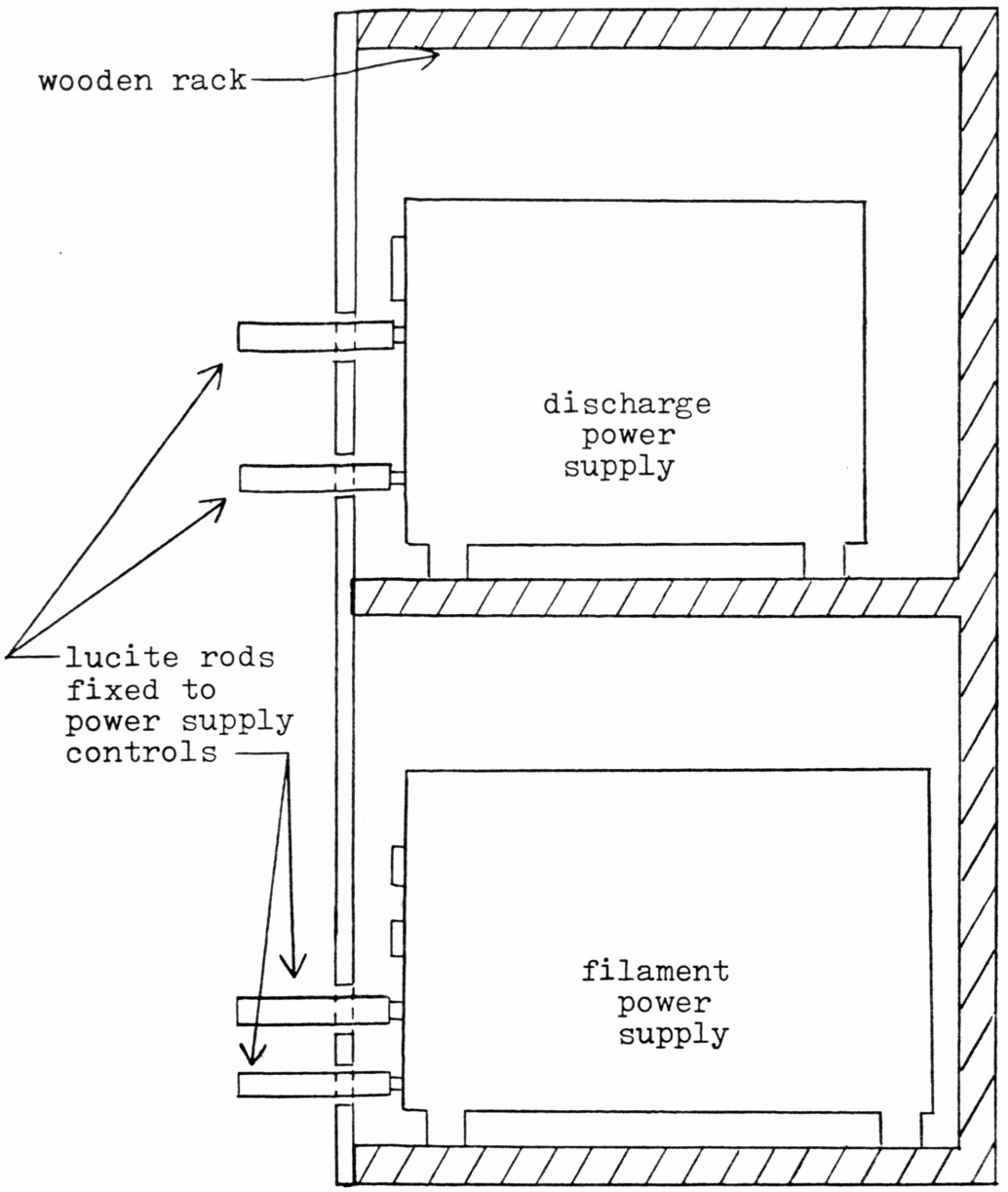

The cases of the ion source power supplies are floated at the accelerating potential and must not be touched. They are encased in a wooden rack which is covered in front with a clear sheet of plexiglass. Adjustment of the control settings can then safely be done with insulating lucite rods.

the ion source. With the extracting electrode at its closest position problems occured with sparking from the ion source to this electrode for extraction voltages above 5 kV. The problem was alleviated by adjusting the position of the electrode to about .35 inches from the ion source exit hole. Only a slight decrease in beam current resulted at the new position. Erosion of the extraction electrode has been observed and is probably due to sputtering, however the erosion is very slight and does not seem to be a problem.

The lens (figure 7) was a 3-element einzel lens, the center element being at positive high voltage with respect to the other two, which were grounded. Each lens element is a brass disk 2 inches in diameter with a 3/4 inch aperture. The elements were seperated by .5 inches using ceramic spacers to prevent leakage from one element to another. These ceramic spacers provided all the mechanical stability needed by the lens. The amount of voltage needed on the center lens element for focussing the beam varied from about 2/3 to 3/4 of the extraction voltage in the range 0-4 kV.

High voltage connection to the center lens element was obtained by putting a high voltage feed through the vacuum wall, which was connected to a rectangular metal plate measuring 1/2 by 2 inches. The plate was mounted against the vacuum wall with the long dimension parallel to the beam. A metal spring which was screwed to the center lens element could then ride against this plate and maintain electrical connection with positional adjustability.

The position of the lens could be adjusted through 1 1/2 inches, with the center of the lens being 1 1/4 inches from the extraction

FIGURE 7
Accelerator and Lens Assembly

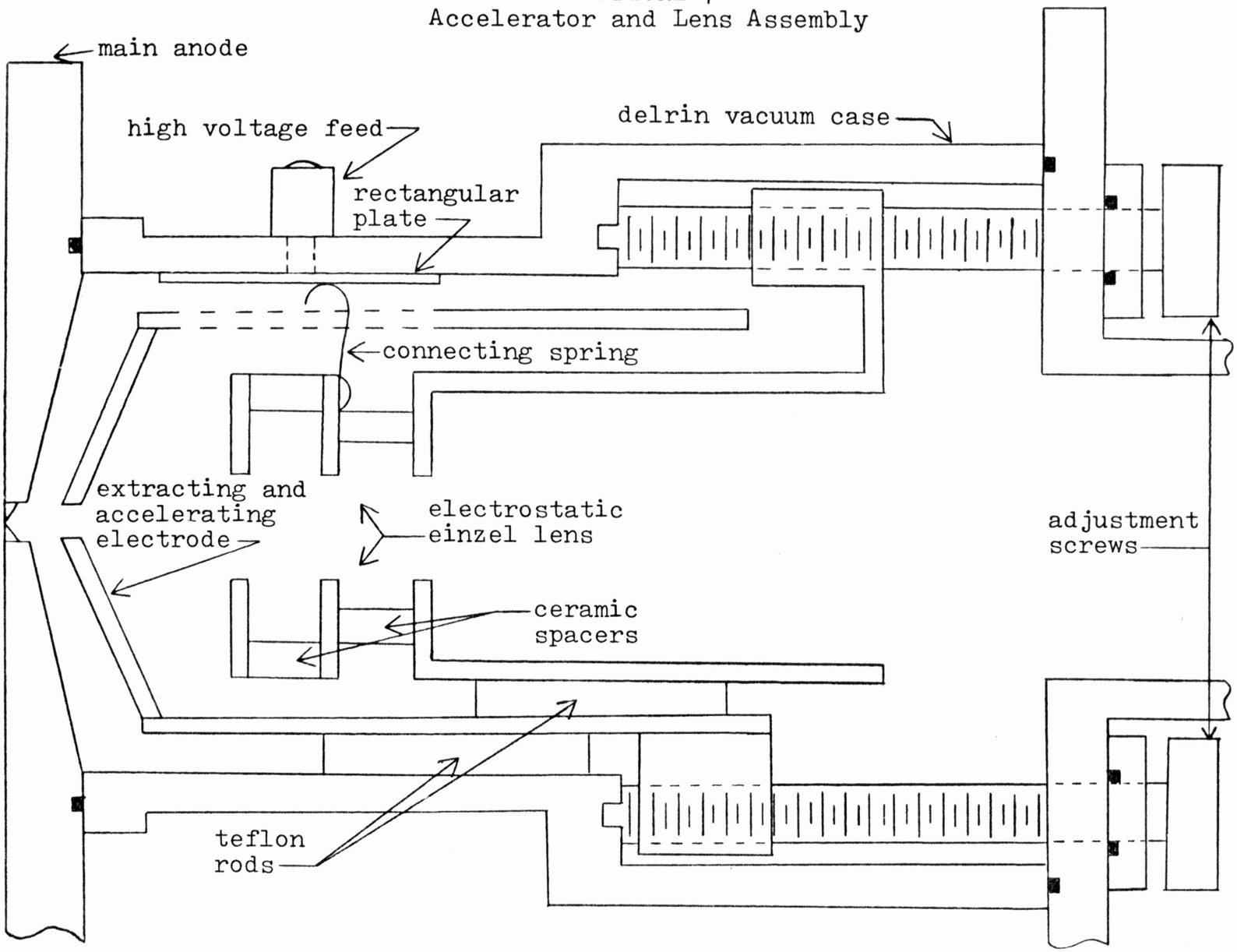

electrode at its closest. Since the transverse magnification of an electrostatic lens is inversely propotional to the object distance, the lens should be kept as far from the extractor as possible. However, one must also sacrifice as little intensity as possible due to loss of solid angle subtended by the lens aperture. Experiments showed the loss of intensity with increasing object distance to be minimal, and the lens position was maintained at 2 1/4 inches from the extraction electrodes throughout this experiment.

In order to adjust the positions of the extraction electrode and the lens both were mounted on brass cylinders as shown in figure 8. The extraction electrode was threaded and screwed into the top of a long cylinder whose inside diameter equaled the outside diameter of the base of the extractor. At the other end of the cylinder was a block which screwed onto the cylinder and which had a threaded hole cut along the direction parallel to the beam axis. Through this threaded hole fit a screw which was allowed freedom to rotate only. The screw extended outside the vacuum wall and could be turned from the outside. Turning the screw thereby caused the cylinder and extractor to move axially. The lens could be adjusted in an identical way. A slot was cut lengthwise in the extraction electrode cylinder so that the high voltage spring on the center lens element could maintain contact with the high voltage plate without shorting. Along the outside of the cylinders were teflon rods, cut to the correct diameters to eliminate the possibility of movement by either cylinder perpendicular to the beam axis. This took the "slop" out the system without causing friction or binding to be a problem. Other than sealing problems at the point where the screws pro-

FIGURE 8
Mounting of Accelerator and Lens

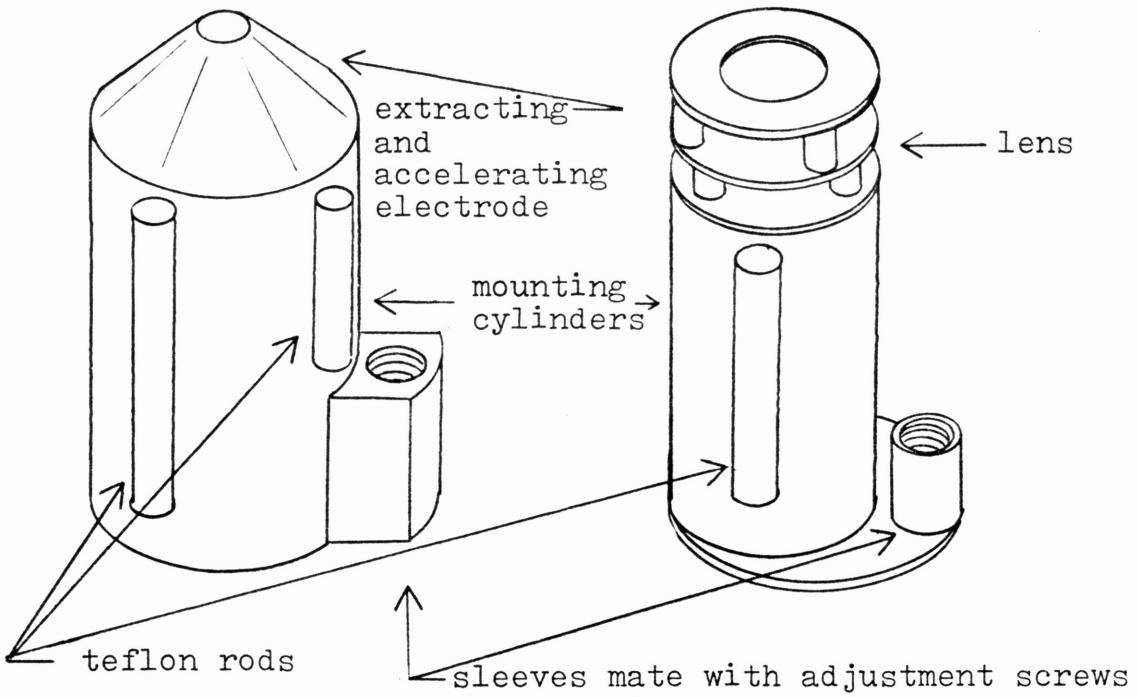

In order to adjust the positions of the accelerating electrode and lens they are mounted on brass cylinders which are attached to threaded sleeves which mate with the adjustment screws. As the adjustment screws are turned from outside of the vacuum system, the cylinders move back and forth along their axes. The teflon rods fit snugly and prevent any transverse motion. For a cross sectional view of these pieces when in place see figure 7.

truded from the vacuum system (which were solved with over sized O-rings) no other difficulties were encountered with this mechanical adjustment design.

Since the entire lens and extraction assembly bolts to the back of the main anode of the ion source (see figure 7) which is at high voltage, the vacuum case was made of the insulating plastic delrin. Delrin is an acetyl homopolymer with a volume resistivity of 10^{15} ohm-cms. and a dielectric strength of 500 V/mil for a 1/8 inch thick section.

Pumping was done with a CVC 2" Blueline diffusion pump model PMCS-2C rated at 105 liters per second. The roughing pump was a Leybold model 6-D.

3. The Collision Chamber

The collision chamber (see figure 9) was constructed with two purposes in mind. First was to examine the beam with a Faraday cup, and secondly as a target chamber for optical measurements. With respect to the first of these, it was desired to be able to reliably locate a Faraday cup at any point along a plane normal to the beam axis. Plane polar coordinates were chosen. Originally, a hollow plexiglass tube, machined round on a lathe, was used as a boom for mounting the Faraday cup. A conductor was fitted through the boom and it was sealed at the end with low vapor pressure epoxy. The Faraday cup was then connected to the conductor and mounted on the inside end of the boom, so that current measurements could be made with a Keithley Instruments model 600B electrometer. The boom was sealed with an O-ring at the point of exit

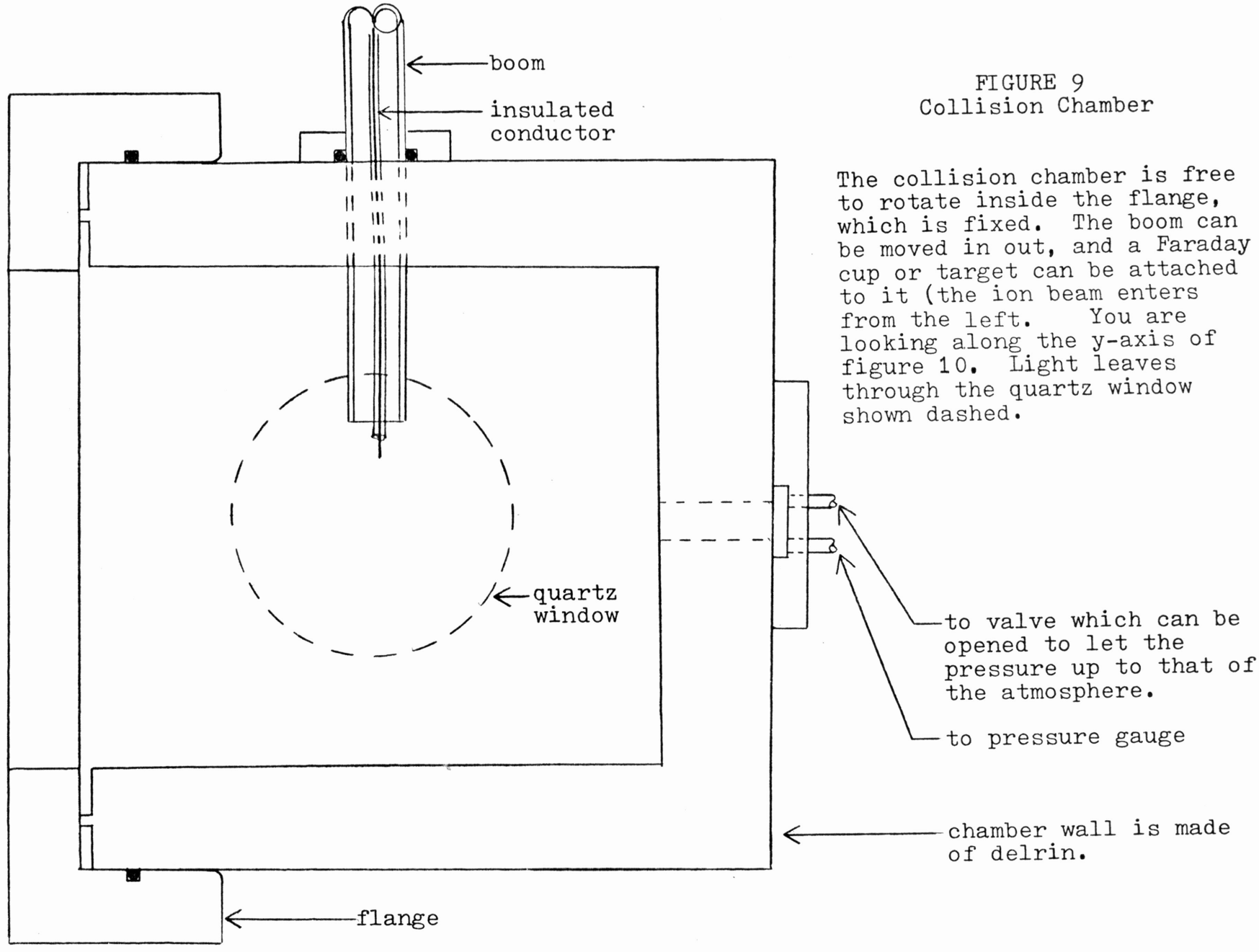

FIGURE 9
Collision Chamber

The collision chamber is free to rotate inside the flange, which is fixed. The boom can be moved in out, and a Faraday cup or target can be attached to it (the ion beam enters from the left. You are looking along the y-axis of figure 10. Light leaves through the quartz window shown dashed.

from the target chamber and could be moved in and out as desired to obtain the radial position of the Faraday cup with respect to the beam axis. The plexiglass lacked the strength necessary, however, and shattered after only a few days of use. It was replaced with a polished copper pipe, which has worked well. But since copper is a conductor, it was necessary to insulate the lead along the inside of the pipe, and to prevent contact of the Faraday cup with the end of the pipe. The Faraday cup was simply a used .22 caliber rat-shot casing which was cleaned in nitric and sulfuric acid.

In order to obtain angular freedom in positioning the Faraday cup, the entire chamber was made to be free to rotate inside the flange to which it is mounted. With the O-ring around the outside of the chamber in the groove on the flange (see figure 9) no leaking took place during rotation of the chamber. For the purpose of optical measurements of deexcitations, a quartz window was built into the side of the collision chamber 90 degrees from the boom. The target consisted of a rectangular aluminum plate measuring 3/4 inches wide by 3 inches long mounted with the long dimension at some small angle from the beam axis (see figure 10). This angle could not be externally adjusted and was left fixed at 5 degrees during the experiment. Because the pressure in the chamber (10^{-5} torr) is too high to maintain a clean metal surface for a reasonable amount of time, the target is covered with a layer of gas (primarily oxygen) atoms. N. H. Tolk and others have found that the oxygen covering on the target surface causes decreased orientation of the beam atoms after collision[3], but increased total intensity[4], and interprets this phenomenon as a change in the deexcitation probabil-

FIGURE 10
Target Geometry

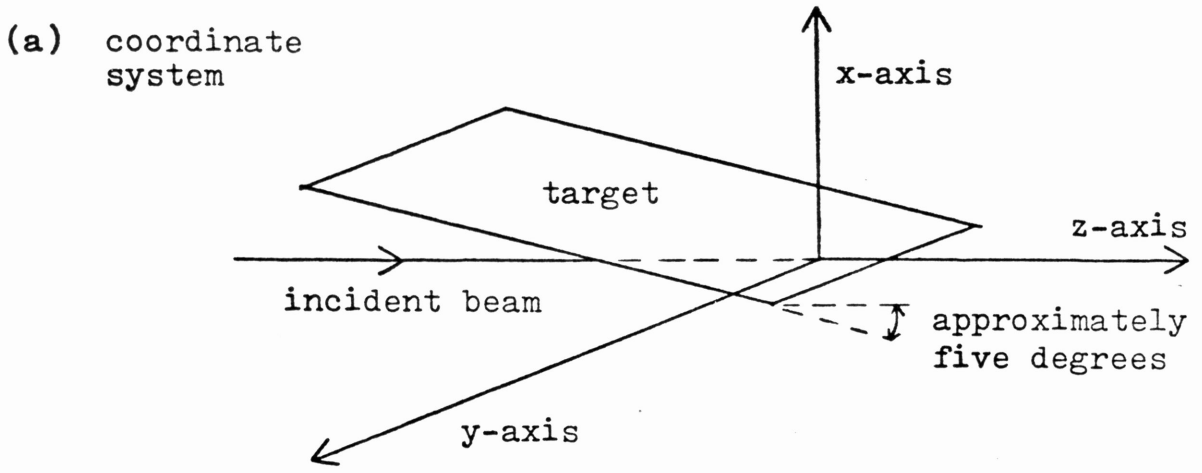

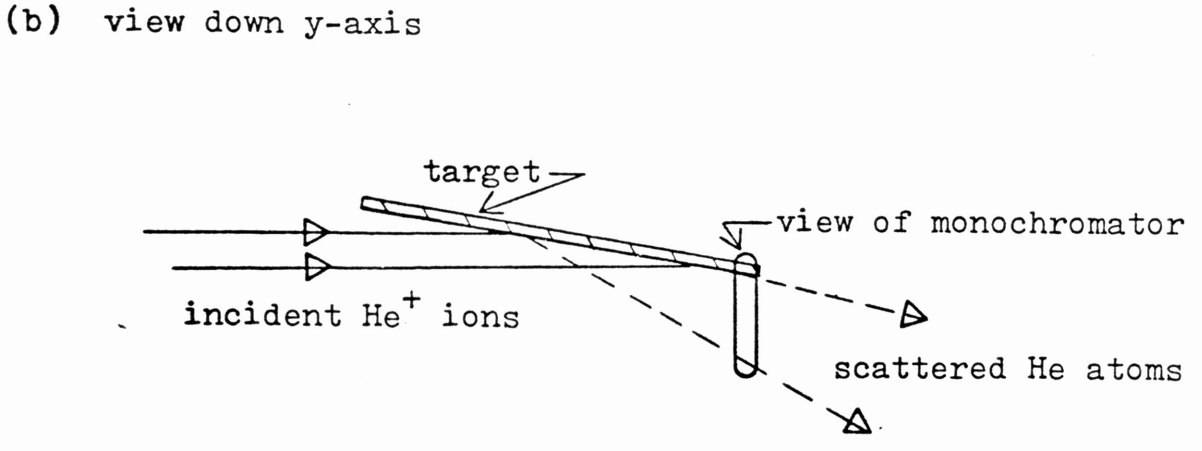

ity near the surface of the target due to the oxygen layer.

4. Optical System

Light was collected from the target region through the window in the collision chamber by the optical system shown in figure 11. All the optical elements were aligned along the y-axis of the coordinate system shown in figure 10. Directly outside the window of the collision chamber was the first lens, which was positioned to collect light from its focal point and transmit it as parallel light through the wavelength adjustable quarter wave plate, and a linear polarizer. The axes of the quarter wave plate made a 45 degree angle with the x and z-axes of figure 10. The axis of polarization of the linear polarizer could be adjusted through 135 degrees. The light transmitted through the linear polarizer was focussed by a second lens onto the entrance slit of a .5 meter f/8.6 Jarrell-Ash model 82-000 Ebert Scanning Monochromator. The wavelength selected light leaving the monochromator fell on the cathode of an EMI-Gencom model 9789QA photomultiplier tube operated in the single-photon counting mode.

The primary goal in the design of the optical system was the measurement of the Stokes parameters of the light emitted by scattered fast atoms or ions from the target. Circular polarization of light emitted by the fast projectiles, when incident on the quarter wave plate, is transmitted as linearly polarized light (see figure 11). Either right circularly polarized light or left circularly polarized light can then be selected for analysis with the linear polarizer. Linearly polarized light can be analyzed by effectively removing the quarter wave plate

FIGURE 11
Optical Arrangement

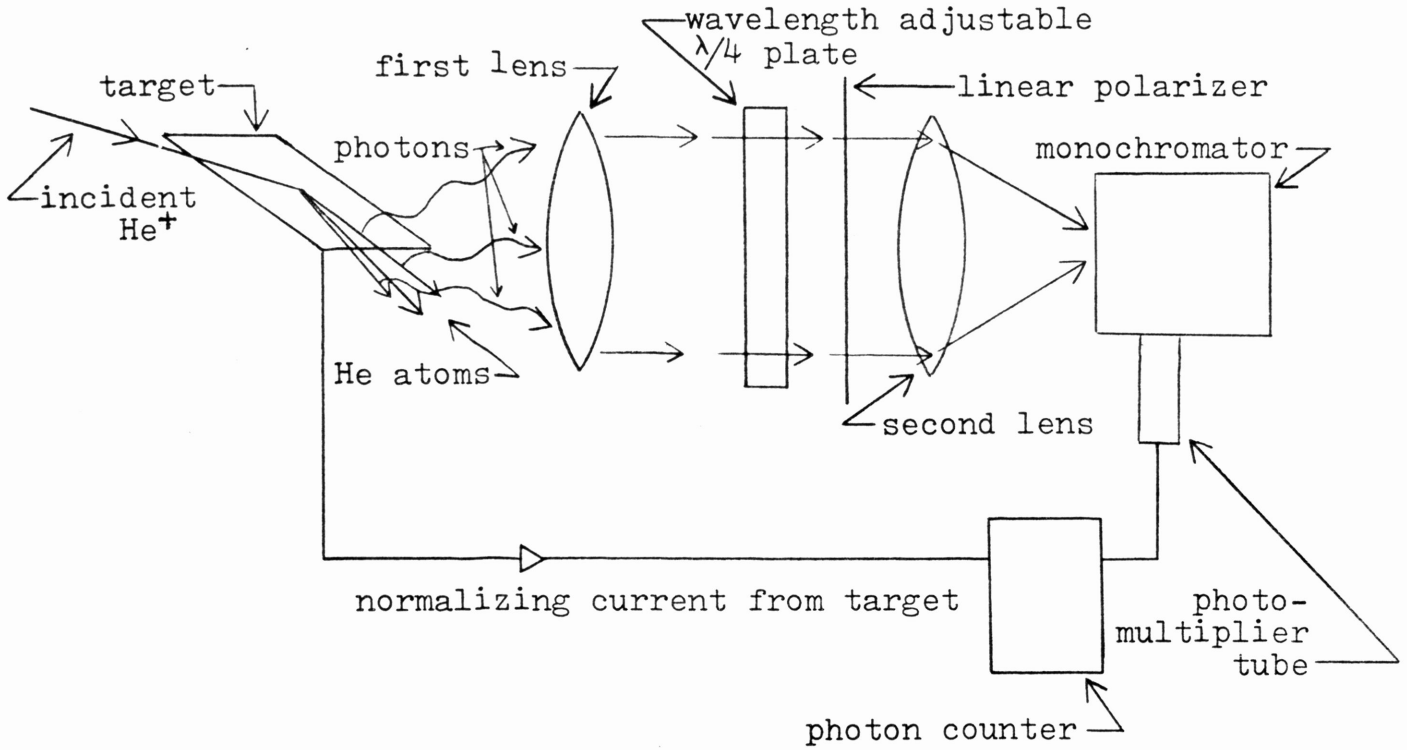

He^+ ions collide with the target and are excited during the collision. After travelling a short distance (typically about 5 mm.) they deexcite, thereby emitting light. The light is gathered by the first lens which is a distance from the target equal to its focal length. The parallel rays pass through a $\lambda/4$ plate whose axes are known. The radiation then passes through a linear polarizer which can be rotated through 135 degrees. Finally the light is focussed by the second lens onto the slit of a monochromator and analyzed according to wavelength. The photons are converted to voltage pulses by the photomultiplier tube and counted by the photon counter. The counting is normalized to the incident beam current.

(see below).

Since the intensities of the light under analysis were quite low (typically only about 100 counts per second from the photomultiplier tube) the optical system was made light tight by enclosing the optical elements in an aluminum tube. However the preceding paragraph implies the need to insert and withdraw a quarter wave plate from the system, and to be able to use a quarter wave plate at several wavelengths. Rather than obtaining a separate such retarder for each wavelength analyzed, and risk swamping the signal with light leaks, a wavelength adjustable quarter wave plate was built into the system[5]. This device consists of a block of fused quartz which can be compressed along an axis perpendicular to the transmitted light ray. When quartz is compressed it becomes birefringent: the amount birefringence increases with the amount of stress. The stress was applied by applying torque to a screw, which pushed a brass block against the quartz. In this way stress was applied evenly on the quartz, and the birefringence could be calibrated to the amount of torque applied. Calibration was done by shining linearly polarized light from a broad-band source into the optical system. The axis of polarization was chosen to be 45 degrees between the slow and fast axes of the retarder. For a given wavelength, the quarter wave condition was satisfied when no change in intensity resulted from a rotation of the linear polarizer behind the quartz block. The torque recuired was recorded for several wavelengths, until a calibration curved was obtained. Therefore, to perform linear polarization measurements, no torque was applied, and no retardation of any component of the ray resulted from the presence of the quartz. To per-

form circular polarization measurements, the screw could be torqued to give quarter wave retardation at whatever wavelength desired. It was determined experimentally that the axis of compression becomes fast with respect to the axis perpendicular to compression. This was done by obtaining a quarter wave plate with the axes marked. The marked quarter wave plate was superimposed over the quartz block which was under compression. Light polarized at 45 degrees between the axes of this composite plate was sent through, and then analyzed with another linear polarizer. When the slow axis of one retarder was parallel to the fast axis of the other retarder, no net retardation of the light resulted, and extinction occured when the linear polarizers were crossed. When the slow axis of one retarder overlapped the slow axis of the other retarder, a half wave plate resulted and extinction occured when the transmission axes of the linear polarizers were parallel.

Since several reflections take place during wavelength analysis inside the monochromator, it is expected that there should be some natural polarization bias inherent in the monochromator. This was in fact observed by transmitting linearly polarized light into the monochromator. Instensity variations were seen as the angle of polarization was changed, but by coincidence the natural polarization bias was zero at 3889 Å, which was the wavelength for which polarization data was taken in this experiment.

5. Electronics

The signal from the photomultiplier tube was preamplified and sent to an Ortec model 474 Timing Filter Amplifier. The output signal was fed into an Ortec model 934 Constant Fraction Discriminator. The out-

put from the discriminator was sent to both an Ortec model 9315 Photon Counter and an Ino-Tech model 5200 Multichannel Analyzer. The output of the constant fraction discriminator is a -800 mV pulse with duration adjustable from less than 6 ns to greater than 150 ns. The input of the multichannel analyzer was specified to be +5 V of greater than 50 ns duration. For this reason an inverting amplifier was constructed consisting of a common emitter transistor arrangement followed by a monostable multivibrator. The output of this device was +5 V of duration adjustable from 0 to 1.7 microseconds. The circuit is shown in figure 12.

The photon counting was normalized to beam current rather than time since low frequency fluctuations persisted in the beam current. To do this, the recorder output of the electrometer used to measure the beam current, which was proportional to the meter deflection, was converted to a counting signal with a Teledyne-Philbrick model 4703 voltage to frequency converter. This signal was fed into the secondary counter input of the photon counter which controlled the counting interval of the main counter. Photon pulses from the photomultiplier tube were counted in the primary counter until a preset value was reached in the secondary counter. In effect, the beam current was time integrated until a standard amount of charge (500 micro-Coulombs in this experiment) had impinged on the target. The number of photons counted was recorded and the counters were reset so the process could begin again. The multichannel analyzer was used to obtain quick estimates of values before actual data taking begain with the photon counter. Background noise counting was done for fixed time intervals rather than for constant current intervals.

FIGURE 12
Inverting Pulse Shaper

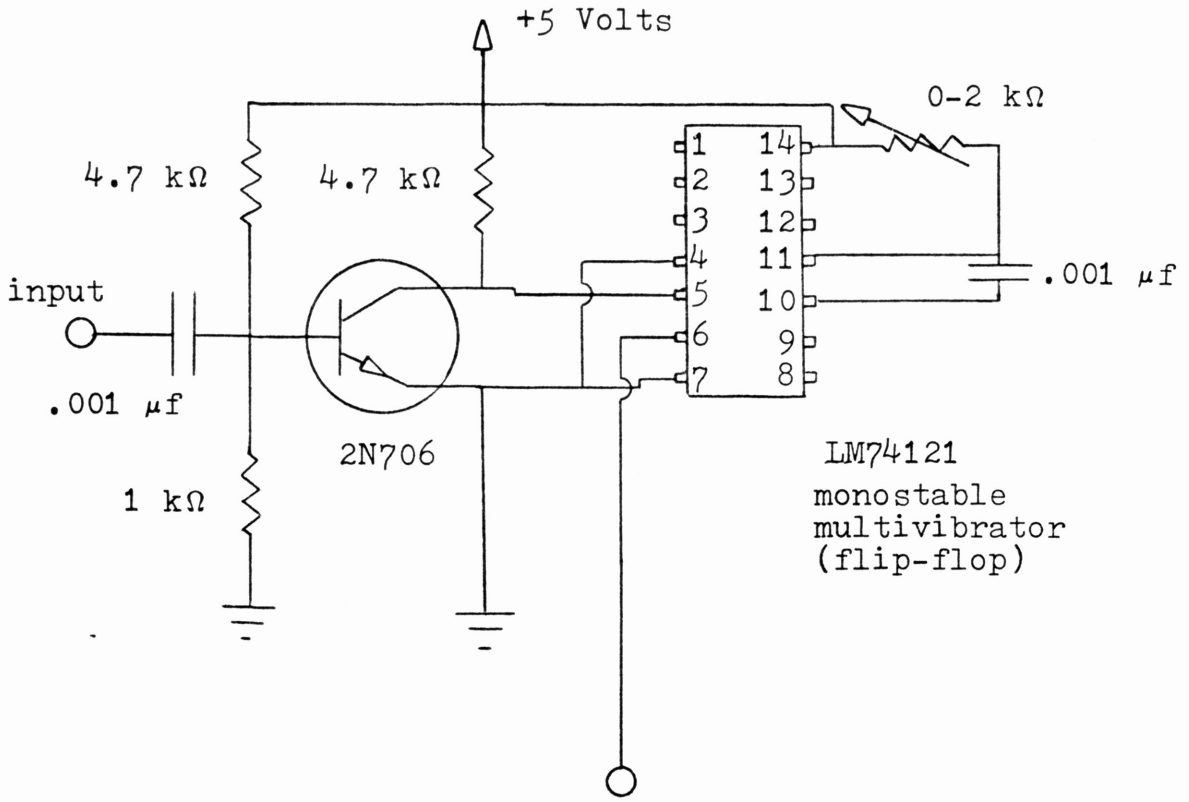

This pulse shaper accepts as input the output of the constant fraction discriminator, (-800mV, 6-150ns) and outputs a nominal 5 Volt positive pulse of 0-1.7μs duration. This output is used to trigger the multi-channel analyzer.

THEORY

The major point of interest in this research was in the anisotropy of the angular momentum distribution of the state of an atom after collision with a target, and thereby a deepened understanding of the actual collision process. Since the apparatus previously described has the primary function of analyzing the polarization of the radiation produced in the vicinity of the target, a theory must be developed for relating this polariztion information to the state of the atoms which are emitting it. Simply by scanning the monochromator through its range of wavelengths, the transitions taking place were obtained by comparision of the wavelengths observed to a helium energy level diagram (see figure 13). The brightest line observed, near 3889 $\mathring{A}$, was the unresolved components of the $2s\ ^3S_1 - 3p\ ^3P_{2,\,1,\,0}$ transition of neutal helium (indicating that charge capture by the incident ion took place during the collision). This was the transition for which polarization data was taken. Although the theory about to be presented is general, the numbers are worked out for this transition only.

Fano and Macek[6] introduce a detector coordinate frame ζ, ξ, η where $\hat{\zeta}$ is the detector direction, $\hat{\xi}$ is the axis of the linear polarizer, and $\hat{\eta}$ is normal to both. They then define two alignment parameters

$$A_o^{det} = \frac{\langle (i' | 3\, J_\zeta^2 - \vec{J}^2 | i) \rangle}{j_i(j_i + 1)}$$

FIGURE 13
Abridged Energy Level Diagram for Neutral Helium

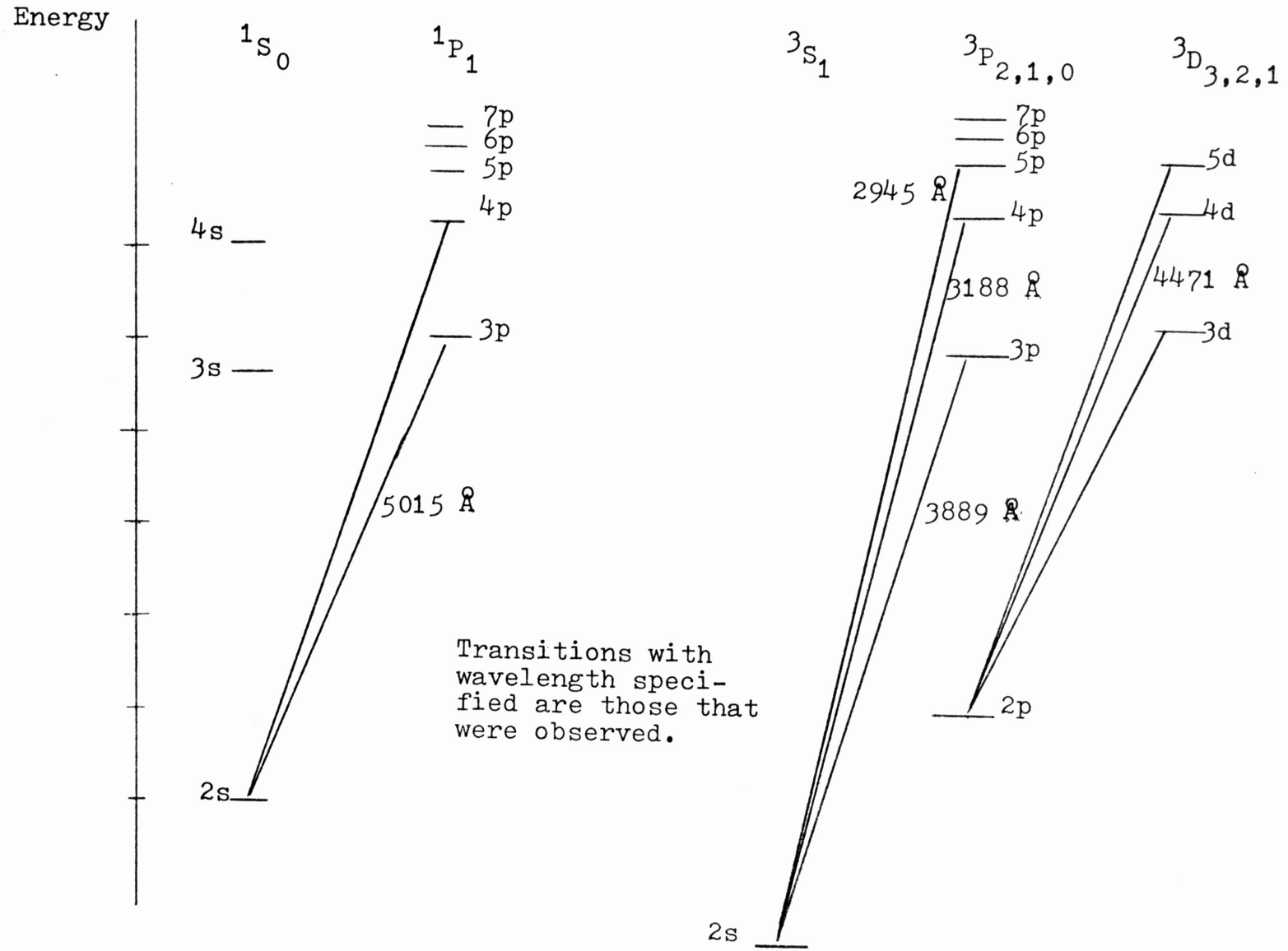

$$A_{2+}^{det} = \frac{\langle (i' | J_\xi^2 - J_\eta^2 | i) \rangle}{j_i(j_i + 1)}$$

and an orientation parameter

$$O_o^{det} = \frac{\langle (i | J_\zeta | i) \rangle}{j_i(j_i + 1)} \quad ,$$

in order to obtain an expression for the measured intensity I. They arrive at

$$\begin{aligned} I = \frac{1}{3} CS \{ 1 &- \tfrac{1}{2} h^{(2)}(j_i, j_f)\, A_o^{det} \\ &+ \tfrac{3}{2} h^{(2)}(j_i, j_f)\, A_{2+}^{det} \cos 2\beta \\ &+ \tfrac{3}{2} h^{(1)}(j_i, j_f)\, O_o^{det} \sin 2\beta \}. \end{aligned} \qquad (1)$$

In this expression, C is a constant depending on wavelength and geometry. S is the average over all directions and polarizations of the emitted radiation. Also in equation (1), the $h^{(k)}(j_f, j_i)$ is a coupling term given by

$$h^{(k)}(j_i, j_f) = (-1)^{j_i - j_f} \frac{\begin{Bmatrix} j_i & j_i & k \\ 1 & 1 & j_f \end{Bmatrix}}{\begin{Bmatrix} j_i & j_i & k \\ 1 & 1 & j_i \end{Bmatrix}} .$$

The terms in braces are standard 6j coefficients and are tabulated by Rotenberg et al.[7]. The term β in equation (1) represents the selection by the detector of linearly or circularly polarized light, with β=0 for

linearly polarized light, $\beta=\pi/4$ for right circularly polarized light, and $\beta=-\pi/4$ for left circularly polarized light. In order to arrive at the orientation and alignment of the atom, which can be related to the collision, the following collision frame is introduced:

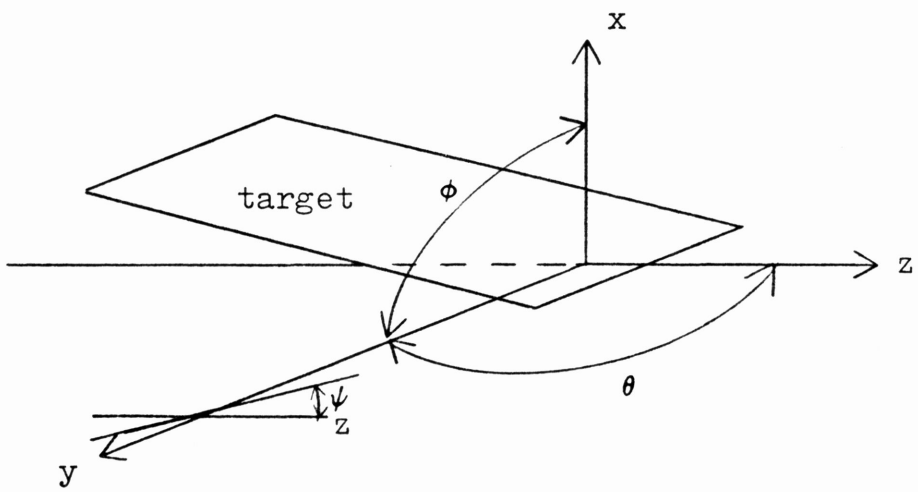

Here, z is the beam direction, θ and ϕ specify the spherical coordinates of the detector (both $\pi/2$ for this experiment), and ψ is the angle of the axis of the linear polarizer with respect to z. Then making the definitions

$$O_{1-}^{Col} = \frac{\langle(i'|J_y|i)\rangle}{j_i(j_i+1)} \qquad (2)$$

$$A_o^{Col} = \frac{\langle (i' | 3J_z^2 - \vec{J}^2 | i) \rangle}{j_i(j_i + 1)}$$

$$A_{1+}^{Col} = \frac{\langle (i' | J_x J_z + J_z J_x | i) \rangle}{j_i(j_i + 1)} \qquad (2)$$

$$A_{2+}^{Col} = \frac{\langle (i' | J_x^2 - J_y^2 | i) \rangle}{j_i(j_i + 1)}$$

the coordinate transformation leads to

$$O_o^{det} = O_{1-}^{Col} \sin\theta \sin\phi$$

$$A_o^{det} = A_o^{Col} \frac{1}{2}(3\cos^2\theta - 1) + A_{1+}^{Col} \frac{3}{2} \sin 2\theta \cos\phi$$

$$+A_{2+}^{Col} \frac{3}{2} \sin^2\theta \cos 2\phi$$

and

(3)

$$A_{2+}^{det} = A_o^{Col} \frac{1}{2} \sin^2\theta \cos 2\psi$$

$$+ A_{1+}^{Col} \{\sin\theta \sin\phi \sin 2\psi$$

$$+ \sin\theta \cos\theta \cos\phi \cos 2\psi\}$$

$$+ A_{2+}^{Col} \{\frac{1}{2}(1 + \cos^2\theta) \cos 2\phi \cos 2\psi$$

$$-\cos\theta \sin 2\phi \sin 2\psi\}.$$

By substituting the values for ϕ and θ into eqs. (3), and then substituting the results into eq. (1) and looking up the 6j symbols for the $^3S_1 - {}^3P_{2,1,0}$ transition, the expressions for $I(\psi)$ are obtained. These are presented in table 1.

The Stokes parameters are defined by

$$\frac{M}{I} = \frac{I_0 - I_{90}}{I_0 + I_{90}}$$

$$\frac{C}{I} = \frac{I_{45} - I_{135}}{I_{45} + I_{135}} \qquad (4)$$

$$\frac{S}{I} = \frac{I_{RCP} - I_{LCP}}{I_{RCP} + I_{LCP}} .$$

Examining the expressions for $I(\psi)$ in table (1) gives the plausible result that

$$I = I_0 + I_{90} = I_{45} + I_{135} = I_{RCP} + I_{LCP}.$$

The Stokes parameters can be obtained by computing the fractional time averaged intensity arising from each J level in the unresolved $2^3S_1 - 3^3P_{2,1,0}$ transition. These fractions are given by Fano and Macek[8] and become

$$\frac{(2J+1)^2}{2S+1} \cdot \begin{Bmatrix} J & J & K \\ L & L & S \end{Bmatrix}^2 .$$

where K = 1 for circular polarization and K = 2 for linear polarization. The numbers are presented in Table 2. Since the transition is unresolved, the intensities given in Table 1 for each J are multiplied

by the fractions in Table 2 for each J before being combined by equations (4) to obtain the relationships for the expressions for the intensities used to compute the Stokes parameters corresponding to the experimental configuration used. The final result is

$$\frac{M}{I} = \frac{-\frac{1}{6} A_0^{Col} + \frac{1}{6} A_{2+}^{Col}}{\frac{5}{9} - \frac{1}{18} A_0^{Col} - \frac{1}{6} A_{2+}^{Col}}$$

$$\frac{C}{I} = \frac{-\frac{1}{3} A_{1+}^{Col}}{\frac{5}{9} - \frac{1}{18} A_0^{Col} - \frac{1}{6} A_{2+}^{Col}}$$

$$\frac{S}{I} = \frac{2O_{1-}^{Col}}{\frac{5}{9} - \frac{1}{18} A_0^{Col} - \frac{1}{6} A_{2+}^{Col}} .$$

RESULTS

Five helium lines were observed in the wavelength range of 5500Å--2000Å. The upper limit of this range was set by the photomultiplier tube response and the lower limit was set by that of the polarizer. The wavelengths of these lines and the corresponding transitions are presented in Table 3. The transitions were obtained from Striganov and Sventitskii[9]. All the transitions are for neutral helium, and the five observed are accepted as the most intense for helium in the wavelength range specified.

The total intensity observed as a function of energy is presented in Graph 1. The intensities are obtained as a number of counts normalized to beam current as described in section 5 under Apparatus. The values are given in terms of multiples of the 1 kV value.

The normalized Stokes parameters M/I, C/I, and S/I were computed from measurements of the intensities of light polarized parallel to, perpendicular to, 45 degrees from, and 135 degrees from the beam axis. The results are presented in graph 2. The error bars represent plus and minus one standard deviation from the mean value. Since each of the normalized Stokes parameters is defined as a ratio, the standard deviation was arrived at by use of the formula

$$\sigma_f = \bar{f}\left[\left(\sigma_1^2/\bar{f}_1^2\right) + \left(\sigma_2^2/\bar{f}_2^2\right)\right]^{1/2}$$

where $f = f_1/f_2$ and σ_1 is the standard deviation of f_1 and σ_2 is the standard deviation of f_2. The fact that the error bars are relatively

GRAPH 1
Total Intensity as
a Function of
Incident Ion Energy

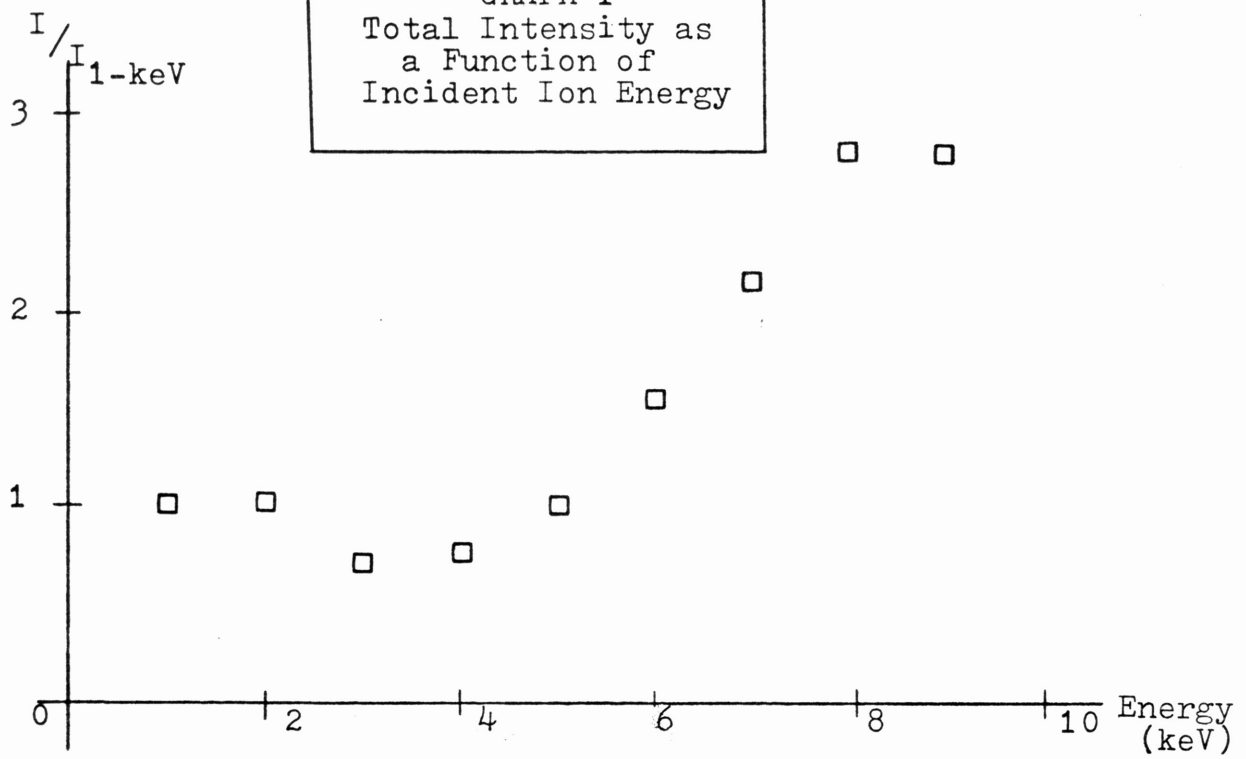

GRAPH 3
Signal-to-Noise Ratio as
a function of
Incident Ion Energy

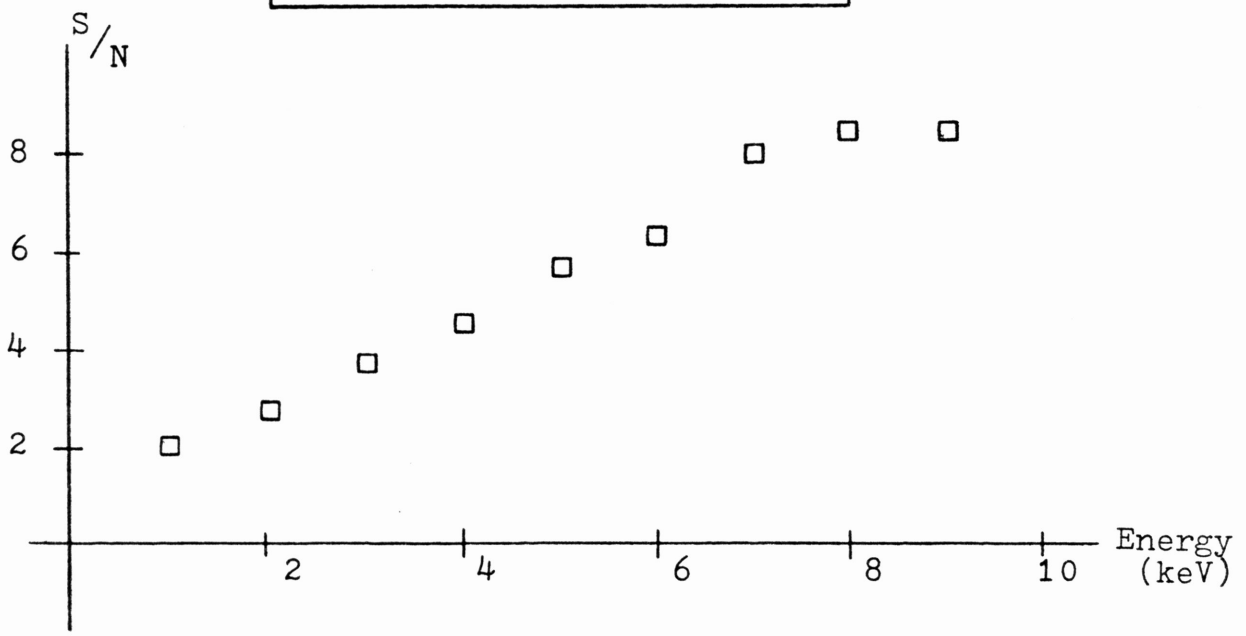

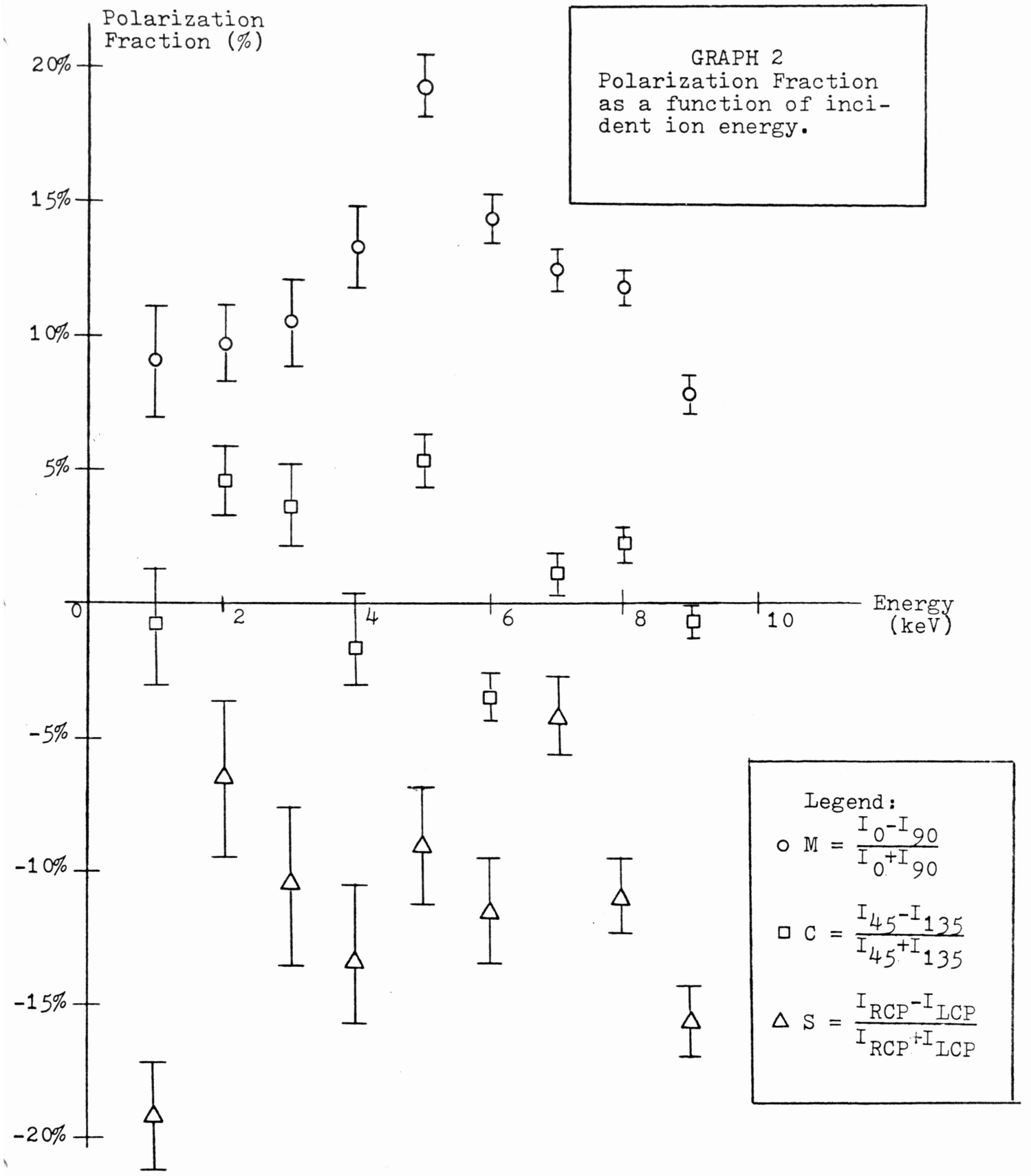
Polarization Fraction (%)
20%
15%
10%
5%
0
-5%
-10%
-15%
-20%
2
4
6
8
10
Energy (keV)
GRAPH 2
Polarization Fraction as a function of incident ion energy.
Legend:
M = $\frac{I_0 - I_{90}}{I_0 + I_{90}}$
C = $\frac{I_{45} - I_{135}}{I_{45} + I_{135}}$
S = $\frac{I_{RCP} - I_{LCP}}{I_{RCP} + I_{LCP}}$

large is due to the low signal to noise ratio from the high background count. It was interesting that the signal to noise ratio was so low, even with the maximum possible beam current of about 40 microamps. The background count was arrived at by turning off the acceleration voltage. It was noticed that even with no acceleration voltage photons were produced by collisions with the target of thermal neutral helium atoms escaping from the ion source. This was verified by two procedures. First the ion source was shut off, and it was observed that the count rate dropped to that of the dark count rate of the photomultiplier tube, verifying that light was being produced by thermal helium escaping from the source. Then with the source running again with no acceleration voltage, a reflection voltage was put on the lens to stop any charged particles which might be escaping and the count rate remained constant. This background light was determined to be unpolarized. A plot of signal to noise ratio versus acceleration voltage is shown in Graph 3.

Since only the 3 Stokes' ratios were measured, the 4 atomic parameters given in equations (5) in the theory cannot be explicitly solved for. However useful considerations can still be made. Equations (5) can be rewritten as

$$\frac{M}{I} = \frac{\frac{3}{10}\left(A_{2+}^{Col} - A_{o}^{Col}\right)}{1 - \frac{1}{10}\left(3A_{2+}^{Col} + A_{o}^{Col}\right)}$$

$$\frac{C}{I} = \frac{-\frac{3}{5} A_{1+}^{Col}}{1 - \frac{1}{10}\left(3A_{2+}^{Col} + A_{o}^{Col}\right)}$$

$$\frac{S}{I} = \frac{\frac{18}{5} O_{1-}^{Col}}{1 - \frac{1}{10}(3A_{2+}^{Col} + A_{o}^{Col})}.$$

Since M/I is positive, $A_{2+}^{Col} > A_{o}^{Col}$. If the assumption is made that A_{2+}^{Col} and A_{o}^{Col} are of opposite sign such that the denominator in the expression is about equal to 1

$$\frac{10}{3} \frac{M}{I} = A_{2+}^{Col} - A_{o}^{Col}.$$

Since values as large as .2 were found for M/I, the difference between A_{2+}^{Col} and A_{o}^{Col} is as large as 2/3, which would be quite suprising if these parameters are of the same sign, thereby supporting the initial assumption. That A_{o}^{Col} and A_{2+}^{Col} are of opposite sign has been supported by the work of D. A. Church[10]. Proceeding with the assumption eqs. (5) become

$$A_{1+}^{Col} = -\frac{5}{3} \frac{C}{I}$$

and

$$O_{1-}^{Col} = \frac{5}{18} \frac{S}{I}$$

which lead to typical values ranging from +1/12 to -1/12 for A_{1+}^{Col} and -1/16 to -1/18 for O_{1-}^{Col}.

CONCLUSIONS

The plots of the Stokes parameters versus incident ion energy shown in Graph 2 show considerable structure. The curve for M/I is roughly bell shaped, peaking at 5 keV, while those for C/I and S/I have several maxima and minima. Since electron capture is taking place in all the observed excitations leading to radiation, it is expected to play an important role in explaining the observed phenomena. The cross section for electron capture in a solid target collision is not known, but investigations of these cross sections for helium ions incident on helium and neon gas have been made in this energy range and it is found that the cross section for exciting the 3^3P state which was under study in this research shows complex structure similar to that seen for the polarization parameters C and S already mentioned[11].

The circular polarization parameter S/I was negative throughout the energy range studied, indicating a dominance of left circularly polarized light. As the incident ion strikes the target, it captures an electron which is at rest in the target when compared to the incident ion velocity. Viewed toward the emitting atom, that is, down the y-axis of the coordinate system presented in figure 10, the electric field vector rotates counter-clockwise. One can interpret this as meaning that the electron was moving in this manner about the nucleus during transition, leading to a picture of the incident atom rolling along the target during the collision. In this way the motion of the electron would add vectorily to zero, which is the initial state of motion of the electron on the surface of the target before being captured by the ion[12]. This

effect has been compared to a billiard ball rolling along a cushion[13].

Tolk has found that for incident ionized atomic and molecular hydrogen, the circular polarization seems to depend on the incident ion energy per nucleon rather than simply on incident ion energy, indicating that the incident particle velocity is a relevent parameter[14]. When the values of S/I obtained in this experiment are analyzed in this manner a very satisfying fit of this data to his curves is seen. Consequently velocity appears in a decisive role for populating this helium p state by capture, even though parameters such as atomic polarization by electric fields are different for hydrogen and helium.

TABLE 1

Intensity as a function of polarization

$J = 0$

$$I_o = \frac{1}{3} CS \{1 - A_o^{Col}\}$$

$$I_{90} = \frac{1}{3} CS \{1 + \frac{1}{2} A_o^{Col} - \frac{3}{2} A_{2+}^{Col}\}$$

$$I_{45} = \frac{1}{3} CS \{1 - \frac{1}{4} A_o^{Col} - \frac{3}{4} A_{2+}^{Col} - \frac{3}{2} A_{1+}^{Col}\}$$

$$I_{135} = \frac{1}{3} CS \{1 - \frac{1}{4} A_o^{Col} - \frac{3}{4} A_{2+}^{Col} + \frac{3}{2} A_{1+}^{Col}\}$$

$$I_{RCP} = \frac{1}{3} CS \{1 - \frac{1}{4} A_o^{Col} - \frac{3}{4} A_{2+}^{Col} + \frac{9}{2} O_{1-}^{Col}\}$$

$$I_{LCP} = \frac{1}{3} CS \{1 - \frac{1}{4} A_o^{Col} - \frac{3}{4} A_{2+}^{Col} - \frac{9}{2} O_{1-}^{Col}\}$$

$J = 1$

$$I_o = \frac{1}{3} CS \{1 + A_o^{Col}\}$$

$$I_{90} = \frac{1}{3} CS \{1 - \frac{1}{2} A_o^{Col} + \frac{3}{2} A_{2+}^{Col}\}$$

$$I_{45} = \frac{1}{3} CS \{1 + \frac{1}{4} A_o^{Col} + \frac{3}{4} A_{2+}^{Col} + \frac{3}{2} A_{1+}^{Col}\}$$

$$I_{135} = \frac{1}{3} CS \{1 + \frac{1}{4} A_o^{Col} + \frac{3}{4} A_{2+}^{Col} - \frac{3}{2} A_{1+}^{Col}\}$$

$$I_{RCP} = \frac{1}{3} CS \{1 + \frac{1}{4} A_o^{Col} + \frac{3}{4} A_{2+}^{Col} + \frac{3}{2} O_{1-}^{Col}\}$$

$$I_{LCP} = \frac{1}{3} CS \{1 + \frac{1}{4} A_o^{Col} + \frac{3}{4} A_{2+}^{Col} - \frac{3}{2} O_{1-}^{Col}\}$$

$J = 0$

$$I_o = I_{90} = I_{45} = I_{135} = I_{RCP} = I_{LCP} = \frac{1}{3} CS$$

TABLE 2

Fractional Time Averaged

Intensity From Each J Level

	J = 2	J = 1	J = 0
K = 1 fraction	$\frac{5}{12}$	$\frac{1}{12}$	0
K = 2 fraction	$\frac{7}{36}$	$\frac{1}{12}$	0

TABLE 3

OBSERVED LINES

Wavelength	Transition
5015 Å	$2s^1S_0 - 3p^1P_1$
4471 Å	$2p^3P_{2,1,0} - 4d^3D_{3,2,1}$
3889 Å	$2s^3S_1 - 3p^3P_{2,1,0}$
3187 Å	$2s^3S_1 - 4p^3P_{2,1,0}$
2945 Å	$2s^3S_1 - 5p^3P_{2,1,0}$

REFERENCES

1. A. R. Hill, A Fine-Focussed Ion Machine with Applications to Implantation, Microscopy and Machining, European Conference on Ion Implantation (Sept., 1970), p. 30.

2. R. Becherer, G. Gautherin, A. Septier. Influence de la Topographie du Champ Magnétique sur les Propriétés D' Une Source du Type Duoplasmatron, Le Journal de Physique et le Radium Physique Appliquée, 23, 123A-125A (1962).

3. N. H. Tolk, J. C. Tully, J. S. Kraus. Elliptic Polarization of Balmer Radiation from Low-Energy Grazing-Incidence Collisions of Hydrogen Ions on Surfaces, Phys. Rev. Lett. 41, 644 (1978).

4. S. Y. Leung, N. H. Tolk, W. Heiland, J. C. Tully, J. S. Kraus, and P. Hill. Optical Radiation from Low-Energy Hydrogen Atomic and Molecular Ion-Surface Collisions, Phys. Rev. A18, 447 (1978).

5. M. N. McDermott and R. Novick, Phys. Rev. 131, 707 (1963).

6. U. Fano and Joseph H. Macek. Impact Excitation and Polarization of the Emitted Light, Rev. Mod. Phys. 45, 557-559 (1973).

7. Manuel Rotenburg, R. Bivens, N. Metropolis, John K. Wooten, Jr., The 3j and 6j Symbols (Cambridge Massachusetts, the Technology Press, 1959).

8. Fano and Macek, p. 568.

9. A. R. Striganov, N. S. Sventitskii, Tables of Spectral Lines of Spectral Lines of Neutral and Ionized Atoms (New York, Plenum Publishing Co., 1968), p. 21.

10. D. A. Church, private conversation, 17 April 1979.

11. L. Muller, F. J. de Heer, Electron Capture Into Excited States by Helium Ions Incident on Noble Gases, Physica, (1970), p. 382.

12. Tolk, p. 645.

13. H. G. Berry, G. Gabrielse, A. E. Livingston. Production of Orientation and Alignment in Heavy-ion--Surface Collisions, Phys. Rev. A16, 1920 (1977).

14. Tolk, p. 645.